Available online at www.sciencedirect.com

Chemical Engineering Research and Design

journal homepage: www.elsevier.com/locate/cherd

Evaluation of CO_2 separation performance with enhanced features of materials – Pebax® 2533 mixed matrix membranes containing ZIF-8-PEI@[P(3)HIm][Tf_2N]

Guoqiang Li[a], *Wojciech Kujawski*[a,*], *Andrius Tonkonogovas*[b], *Katarzyna Knozowska*[a], *Joanna Kujawa*[a], *Ewa Olewnik-Kruszkowska*[a], *Nerijus Pedišius*[b], *Arūnas Stankevičius*[b]

[a] *Nicolaus Copernicus University in Toruń, Faculty of Chemistry, 7 Gagarina Street, 87-100 Toruń, Poland*
[b] *Lithuanian Energy Institute, 3 Breslaujos Street, Kaunas 44403, Lithuania*

ARTICLE INFO

Article history:
Received 17 February 2022
Received in revised form 7 March 2022
Accepted 14 March 2022
Available online 17 March 2022

Keywords:
MMMs
ZIF-8
Ionic liquids
Post-synthetic modification
CO_2 capture

ABSTRACT

Zeolitic imidazolate framework (ZIF-8) was functionalized by polyethyleneimine (PEI) and subsequently decorated with ionic liquid (IL) – [P(3)HIm][Tf_2N]. ZIF-8-PEI@IL/Pebax® 2533 mixed matrix membranes (MMMs) were fabricated to enhance the CO_2 capture performance of Pebax membranes. The amino groups and IL in ZIF-8-PEI improved the gas separation performance of the MMMs due to the additional CO_2 transporting pathways by using the reversible reaction with amino groups and the high affinity between IL and CO_2. The modified ZIF-8 particles demonstrated enhanced interfacial interactions and compatibility between fillers and polymer matrix due to the presence of amino groups and IL, confirmed by the enhanced gas separation performance, improved elongation at break, and tensile strength of MMMs. Comparing with the pristine membranes, CO_2 permeability of MMMs containing 15 wt% ZIF-8-PEI@IL increased by 123% to 285 Barrer, and the CO_2/N_2 and CO_2/CH_4 ideal selectivity increased from 17 and 12 to 76 and 25, respectively.

© 2022 Institution of Chemical Engineers. Published by Elsevier Ltd. All rights reserved.

1. Introduction

CO_2 separation plays a critical role in environment protection, the development of green energy and energy security (Cui et al., 2021; Kujawski et al., 2020; Gouveia et al., 2021). In comparison to the traditional CO_2 capture technologies, *e.g.* pressure-swing adsorption (Abd et al., 2021), amine absorption (Ji et al., 2021) and cryogenic distillation (Yousef et al., 2018), membrane technology is gaining more and more attention owing to its lower energy consumption, higher flexibility, smaller footprint, and higher efficiency (Liu et al., 2021; Li et al., 2021a).

Pebax® 2533 is a thermoplastic elastomer containing 20 wt % of polyamide (PA) aliphatic hard block providing mechanical strength and 80 wt% of amorphous polyether (PE) soft block facilitating the transport of CO_2 molecules. Pebax® 2533 is regarded as a promising material for the fabrication of membranes for CO_2 separation processes, showing acceptable CO_2 permeability with desirable CO_2/N_2 selectivity (Li et al., 2021a; Kim et al., 2020). However, the properties of polymeric membranes are restricted by the typical trade-off relation between gas permeability and selectivity, expressed by the Robeson upper bound (Dal-Cin et al., 2008). The fabrication of mixed matrix membranes (MMMs) is an efficient way to overcome the trade-off relation in polymeric membranes applied in gas separation processes (Kamble et al., 2021; Singh et al., 2021; Shah Buddin and Ahmad, 2021). MMMs could integrate the processability of polymer matrix and the

* Corresponding author.
E-mail address: kujawski@chem.umk.pl (W. Kujawski).
https://doi.org/10.1016/j.cherd.2022.03.023
0263-8762/© 2022 Institution of Chemical Engineers. Published by Elsevier Ltd. All rights reserved.

excellent gas transport and selective properties of fillers, resulting in both higher gas permeability and better selectivity (Shah Buddin and Ahmad, 2021; He et al., 2022).

Metal organic frameworks (MOFs) have been intensively utilized as fillers in MMMs for enhancing gas separation performance owing to their large surface area, inorganic-organic structural properties and the possible tuning functionality (Wu et al., 2021). Among various types of MOFs, zeolitic imidazolate framework (ZIF-8) consisting of zinc ion centers coordinated with 2-methyl imidazolate has drawn attention in CO_2 separation due to its intrinsic properties and the small aperture equal to 3.4 Å which is bigger than the kinetic diameter of CO_2 (3.3 Å) but smaller than the kinetic diameter of N_2 (3.6 Å) and CH_4 (3.8 Å) (Chi et al., 2015; Nafisi and Hägg, 2014a). Nafisi and Hägg (Nafisi and Hägg, 2014b) prepared ZIF-8 Pebax® 2533 MMMs for CO_2 separation. It was found that with the increase of ZIF-8 content, the CO_2 permeability increased while the CO_2/N_2 selectivity decreased. The decreasing selectivity in MMMs containing ZIF-8 is related to the poor compatibility between ZIF-8 and polymer matrix, resulting in the formation of interfacial voids and defects (Zheng et al., 2019).

To fabricate ZIF-8 incorporated MMMs with higher CO_2 permeability and selectivity, it is crucial to modify ZIF-8 with CO_2-philic groups (Song et al., 2021). Moreover, the modified ZIF-8 can improve the compatibility between filler and polymer matrix due to the enhanced intermolecular interaction, *e.g.*, hydrogen bond (Nordin et al., 2015; Ding et al., 2020; Zhu et al., 2021). Atash Jameh et al. (2020) modified ZIF-8 with ethylenediamine (ED) and prepared Pebax® 1074/ED-ZIF-8 MMMs. It was found that there was not any agglomeration observed when 30 wt% of ED-ZIF-8 was incorporated into MMMs in comparison to 20 wt% for ZIF-8. At the filler content of 30 wt%, Pebax® 1074/ED-ZIF-8 MMMs showed CO_2 permeability equal to 344 Barrer and ideal CO_2/CH_4 selectivity equal to 24.2 which were 157% and 69%, respectively, higher than those for Pebax® 1074/ZIF-8 MMMs. The enhanced gas separation performance for MMMs containing modified ZIF-8 was related to the high affinity of ED for CO_2, resulting in the increased CO_2/CH_4 selectivity. Lv et al. (2021) synthesized bio-inspired ZIF (Bio-ZIF) by introducing amino groups into ZIF-8 *via* the ligand exchange reaction between 3-amino-1,2,4-triazole (Atz) and Hmin of ZIF-8 *via* post-synthetic modification method. The synthesized Bio-ZIF was incorporated into Pebax® 1657 to prepare MMMs for CO_2 separation. When 12 wt% Bio-ZIF was incorporated, the prepared MMMs exhibited high CO_2 permeability equal to 542 Barrer and high CO_2/CH_4 selectivity equal to 40, which surpassed the 2008 Robert upper bound (Lv et al., 2021). This is because the amino groups in Bio-ZIF can react with CO_2 to form zwitterion as an intermediate during the reversible reaction, resulting in the increase of CO_2 permeability.

As discussed above, the CO_2 affinity of ZIF-8 and the compatibility between ZIF-8 and polymer matrix could be enhanced by introducing amino groups into ZIF-8. It is hypothesized that the increase of the number of amino groups in the modifier might further enhance these properties for ZIF-8. Therefore, Jiao et al. (2021) synthesized polyethyleneimine (PEI) functionalized ZIF-8 (PEI-ZIF-8) *via in-situ* method by using Hmin and PEI mixed linker. The prepared PEI-ZIF-8 was incorporated into Pebax® 1657 matrix for MMMs preparation. It was found that the MMMs with 5 wt% PEI-ZIF-8 exhibited CO_2 permeance of 13 GPU (Gas Permeation Unit, 1 GPU = 10^{-6} cm^3(STP)/(cm^2 s cmHg)) and CO_2/N_2 selectivity of 49 which were much higher than the pristine membranes. The improved gas separation performance for MMMs was ascribed to the porous structure and higher affinity with CO_2 of PEI-ZIF-8, the large density of amine groups from PEI providing facilitated CO_2 transport path and enhancing interfacial compatibility.

Ionic liquids (ILs) have been used as additives and gas carriers for the improvement of gas separation performance of membranes due to their preferential solubility of CO_2 over N_2 and CH_4 and low volatility (Rynkowska et al., 2018; Hao et al., 2013). To enhance the interfacial adhesion between fillers and polymer matrix and avoid the formation of non-selective interfacial voids, Li et al. (2016) synthesized ZIF-8 and confined ionic liquid (IL) 1-butyl-3-methylimidazolum bis(trifluoromethylsulfonyl)imide ([bmim][Tf_2N]) into ZIF-8 cages. It was found that the gas separation performance and the mechanical properties of IL@ZIF-8/Pebax® 1657 MMMs were simultaneously improved.

Both the PEI modification and the ionic liquid decoration can improve the gas separation performance and enhance the compatibility between fillers and polymer matrix. Therefore, in this work, the PEI modification and the ionic liquid decoration are combined to modify ZIF-8. The PEI modified ZIF-8 will be decorated with ionic liquid 1-allyl-3 H-imidazolium bis(trifluoromethanesulfonyl)imide ([P(3)HIm][Tf_2N]) owing to its high CO_2 solubility and its role as a sealant to optimize the interfacial morphology between polymer matrix and nanofillers (Nath and Henni, 2020). The prepared ZIF-8-PEI@IL particles will be incorporated into Pebax® 2533 matrix for MMMs preparation to improve the gas separation performance. The amino groups from PEI will provide facilitated CO_2 transport path and enhance the compatibility between filler and polymer matrix *via* hydrogen bond with Pebax® 2533. Moreover, PEI polymer chains located on ZIF-8 could prevent the excessive occupation of IL in ZIF-8. The reduced pore volume and aperture size of the modified ZIF-8 should modulate the gas transporting pathways of the prepared MMMs.

2. Experimental

2.1. Materials

Zinc nitrate hexahydrate ($Zn(NO_3)_2{\cdot}6H_2O$, 98%), 2-methylimidazole (Hmin, 99%), N,N-dimethylformamide (DMF), and branched polyethyleneimine (PEI, 25000 Mw) (Fig. S1a) were purchased from Sigma Aldrich (Poznań, Poland). Methanol (99.8%) and ethanol (99.8%) were purchased from Alchem Grupa Sp. z o.o. (Toruń, Poland).

Ionic liquid of 1-allyl-3H-imidazolium bis(trifluoromethanesulfonyl)imide ([P(3)HIm][Tf_2N], 99%) (Fig. S1b) was purchased from SOLVIONIC (Toulouse, France).

Pebax® 2533 (80 wt% of poly(ethylene oxide) – PEO block and 20 wt% of polyamide – PA-12 block) was kindly provided by Arkema (Colombes, France).

2.2. Synthesis of ZIF-8, ZIF-8-PEI, and ZIF-8-PEI@IL

ZIF-8 was synthesized according to the modified method reported by Wee et al. (2013). 11.75 g of $Zn(NO_3)_2{\cdot}6\ H_2O$ and 25.92 g of 2-methylimidazole were dissolved in 200 mL of DMF. The 2-methylimidazole solution was added into zinc nitrate solution under strong stirring for 10 min. After mixing, the spontaneous precipitation was observed. The

mixture solution was transferred into a 1 L Schott bottle and placed in oven for 4 h at 140 °C (Fig. S2). Subsequently, the temperature of the mixture decreased to room temperature. The as-synthesized product was collected by centrifugation. The obtained products were repeatedly washed three times by dispersing in DMF and ethanol in an ultrasonic bath and recovered by centrifugation. Finally, the obtained products were dried at 100 °C.

ZIF-8 was modified with PEI *via* wet impregnation strategy (Xian et al., 2015). ZIF-8 was heated at 150 °C for 12 h to remove adsorbed and coordinated water. 0.25 g PEI was dissolved in anhydrous 10 mL methanol by stirring and sonication. Then, 1 g ZIF-8 was slowly added into PEI solution under stirring for 30 min. After that, the obtained gel was allowed to stand overnight at room temperature. The final product ZIF-8-PEI was dried in an oven for 12 h at 100 °C (Fig. S2).

To synthesize ZIF-8-PEI@IL, 0.5 g [P(3)HIm][Tf_2N] was dissolved in 15 g anhydrous ethanol to obtain IL solution. Then, 0.5 g ZIF-8-PEI was added to the IL solution to react with IL under stirring at 80 °C for 12 h (Fig. S2). The obtained ZIF-8-PEI@IL was collected *via* centrifugation and washed three times with ethanol and dried in an oven at 100 °C for 12 h.

2.3. Membrane fabrication

ZIF-8-PEI@IL/Pebax® 2533 MMMs were prepared by using the solution casting and solvent evaporation method. First of all, ZIF-8-PEI@IL (0.15 g, 0.3 g, 0.45 g, or 0.6 g) was dispersed in ethanol (90 wt%)/water (10 wt%) solvent homogeneously under strong stirring at 80 °C for 1 h followed by a sonication for 30 min. Pebax® 2533 (3 g) pellets were dissolved in the ZIF-8-PEI@IL suspension in two steps. In the first step, a small amount of Pebax® 2533 pellets were dissolved under strong stirring at 80 °C for 3 h. In the second step, the rest of Pebax® 2533 pellets were added into the above solution under stirring at 80 °C for 12 h to obtain the final 6 wt% Pebax® 2533 solution containing filler. The determined amount of obtained solution was poured into a clean Teflon dish with a glass cover to allow the slow solvent evaporation. The cast membrane was left at room temperature for 3 days, dried at 60 °C following overnight, and then peeled off from Teflon dish (Fig. S3). For the comparison, ZIF-8/Pebax® 2533 and ZIF-8-PEI/Pebax® 2533 MMMs and pristine Pebax® 2533 membranes were prepared following the same procedure.

2.4. Characterization of fillers and membranes

The morphologies of prepared nanoparticles and membranes were characterized by using Scanning Electron Microscope (SEM), applying LEO 1430 VP microscope (Leo Electron Microscopy Ltd., Cambridge, UK) at 30 keV. ImageJ software was used to evaluate the particle size and membrane thickness from SEM pictures.

The pristine and modified ZIF-8 were characterized by using scanning transmission electron microscopy (STEM) with HAADF detector (FEI Europe B.V, Eindhoven, the Netherlands).

Fourier Transform Infrared-Attenuated Total Reflectance (FTIR-ATR) spectra of prepared nanoparticles and membranes were obtained by using Nicolet iS10 (Thermal Scientific, Waltham, USA) spectrometer in the range of 400–4000 cm^{-1}. All obtained spectra were analyzed using Omnic 9 software (Thermo Fisher Scientific, Waltham, USA).

X-Ray Diffraction (XRD) analyses for the pristine and modified ZIF-8 were conducted by utilizing Philips X'Pert (Malvern Panalytical, Malvern, UK). The transmission mode and 2θ range of 5–80° were applied. The X'Celerator Scientific detector (Malvern Panalytical, Malvern, UK) with Cu anode was used.

The nitrogen adsorption/desorption measurements for the pristine and modified ZIF-8 were conducted at –195.7 °C *via* Gemini VI (Micromeritics Instrument Corp., Norcross, GA, USA). All samples were degassed for 6 h at 110 °C before the measurements.

Thermal properties of the prepared nanoparticles and membranes were characterized by using a Jupiter STA 449 F5 (Netzsch, Germany) thermogravimetric analyzer. Thermogravimetric analysis (TGA) measurements were performed in the temperature range of 25–950 °C with heating rate of 10 °C/min under the nitrogen atmosphere. Moreover, the FTIR Vertex 70 V spectrometer (Bruker Optik, Germany) was combined with TGA analysis for nanoparticles to analyze gas products online.

Mechanical properties of the prepared membranes were measured by using the mechanical testing equipment (Shimadzu EZ-Test ZE-SX, Shimadzu, Kyoto, Japan). The prepared samples were placed between two clips. The initial force and the testing speed are 0.1 N and 1 cm/min, respectively. The obtained results were used to determine the tensile strength (MPa) and elongation at break (%) by using the Trapezium X Texture software.

2.5. Gas permeation measurements

The gas permeation tests for pure gas of CO_2, N_2, CH_4, and H_2 were conducted at 2 bar and temperature of 24, 35, 40 and 45 °C by using a home-made equipment which has been described in detail elsewhere (Yousef et al., 2021). The effective membrane area in the module is 12.56 cm^2. Each membrane sample was measured 3 times under stabilized condition for better accuracy. The gas flow rate was recorded by using a bubble flow meter. The gas permeability P (1 Barrer = 10^{-10} cm^3 (STP) cm cm^{-2} s^{-1} $cmHg^{-1}$) was calculated by using Eq. (1) (Jiao et al., 2021):

$$P = \frac{Ql}{\Delta pA} \quad (1)$$

where Q is the gas flow rate (cm^3(STP)/s); l is the membrane thickness (cm); Δp is the pressure difference across the membrane (cmHg); A is the active membrane area (cm^2) (Jiao et al., 2021; Gao et al., 2020).

The ideal selectivity α_{12} was calculated by using Eq. (2) (Li et al., 2021a):

$$\alpha_{12} = \frac{P_1}{P_2} \quad (2)$$

3. Results and discussion

3.1. Characterization of modified ZIF-8

The morphology of ZIF-8, ZIF-8-PEI, and ZIF-8-PEI@IL was investigated by SEM, STEM and TEM techniques and results are shown in Figs. 1 and S4. The synthesized ZIF-8 particles possessed rhombic dodecahedron morphology (Fig. 1). After PEI modification and IL decoration, the edges between particles have been weakened, indicating the successful

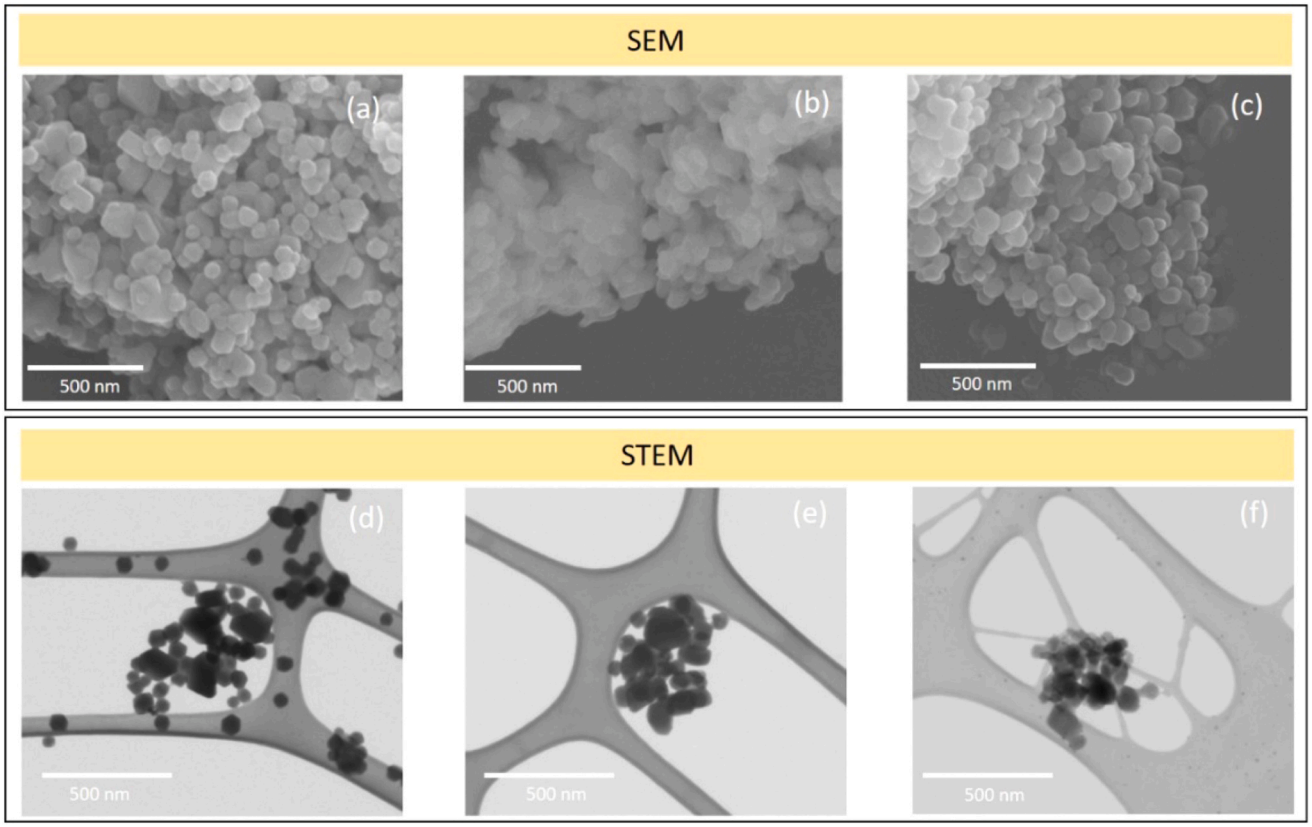

Fig. 1 – SEM and STEM images of ZIF-8 (a, d), ZIF-8-PEI (b, e), and ZIF-8-PEI@IL (c, f).

attachment of PEI polymer chains and decoration of IL as lubricant between ZIF-8 particles (Fig. S4). The morphology of ZIF-8 particles was barely changed after PEI modification and IL decoration. The pristine and modified ZIF-8 particles possess a particle size of 80 – 190 nm evaluated from SEM images by using ImageJ software. The PEI modification and IL decoration barely changed the particle size of ZIF-8. The particle size was also measured by using dynamic light scattering (DLS) technique. As shown in Fig. S5, the average particle size of ZIF-8, ZIF-8-PEI, and ZIF-8-PEI@IL are 115 nm, 424 nm, and 499 nm, respectively, along with the range of particle size distribution of 80–160 nm, 360–750 nm, and 424–750 nm, respectively. For ZIF-8-PEI, and ZIF-8-PEI@IL, the particle size measured by using DLS is larger than that measured from SEM image. This is because DLS measures the hydrodynamic size which is the size of the nanoparticle together with the solvation layer around the particle (Anderson et al., 2013). According to the element analysis by using Energy Dispersive X-Ray Analysis (EDX) mapping (Fig. S6), the F and S elements from [P(3)HIm][Tf_2N] were found in ZIF-8-PEI@IL particles, indicating the successful decoration of IL on ZIF-8.

XRD measurements were conducted to investigate the crystal structure of the pristine and modified ZIF-8. As shown in Fig. 2, the characteristic peaks of ZIF-8 were also found in ZIF-8-PEI and ZIF-8-PEI@IL, indicating that the crystal structure of ZIF-8 was preserved after the PEI modification and IL decoration. However, the intensity of the characteristic peaks of ZIF-8 gradually decreased after the PEI modification and IL decoration owing to the decrease of electron density resulting from the presence of PEI polymer chains and IL in the cage and on the surface of ZIF-8 (Liu et al., 2020). On the other hand, the decrease of surface area (Table S1) and the slight change of the morphology of ZIF-8-PEI and ZIF-8-PEI@IL (Figs. 1b, c and S4e, f) could also result in the decrease of peak intensity (Inoue and Hirasawa, 2013).

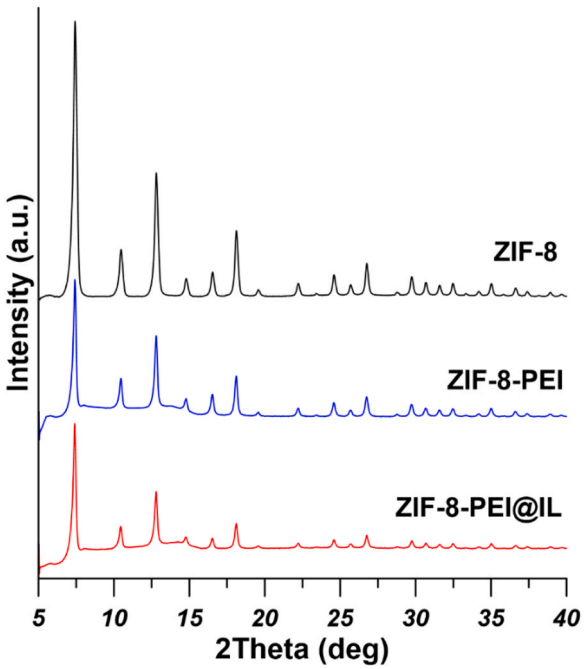

Fig. 2 – XRD patterns of ZIF-8, ZIF-8-PEI, and ZIF-8-PEI@IL.

The N_2 adsorption and desorption isotherms and the particle size distribution of ZIF-8, ZIF-8-PEI, and ZIF-8-PEI@IL were presented in Figs. 3 and S7. The pristine and modified ZIF-8 exhibited the type-I adsorption behavior, indicating the microporous structure of the prepared fillers (ALOthman, 2012; Leofanti et al., 1998). The microporous structure of ZIF-8 was preserved after the PEI surface modification and ILs

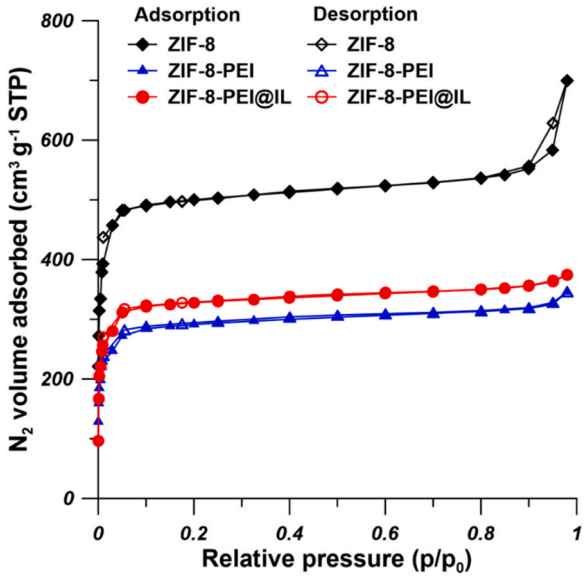

Fig. 3 – N_2 adsorption and desorption isotherms of ZIF-8, ZIF-8-PEI, and ZIF-8-PEI@IL at 77 K.

decoration, which is consistent with the previous reported studies (Li et al., 2016; Menezes et al., 2020). As it is shown in Table S1, the Brunauer, Emmett and Teller (BET) surface area, total pore volume, micropore volume and average pore size of synthesized ZIF-8 are comparable with the previous literatures (Zheng et al., 2019; Jiao et al., 2021; Menezes et al., 2020). For ZIF-8-PEI, the BET surface area, total pore volume and average pore size decreased due to the impregnation of PEI in ZIF-8. Jiao et al. (2021) also found the decrease of BET surface area from 1628.8 m^2/g to 998.0 m^2/g after the PEI modification for ZIF-8. For ZIF-8-PEI@IL, the BET surface area, total pore volume and average pore size are comparable to ZIF-8-PEI. Further investigation on the micropore volume and mesopore volume (Table S1) showed that the increase of total volume was mainly determined by the increase of mesopore volume, since the micropore volume barely changed. The PEI chains in the mesopore was replaced by ILs resulting in the increase of mesopore volume since the size of ILs is smaller than PEI.

The FTIR spectra were used to characterize the chemical structure of ZIF-8, ZIF-8-PEI, and ZIF-8-PEI@IL (Fig. 4). For pristine ZIF-8, the peaks at 3135 cm^{-1} and in the range of 3000–2800 cm^{-1} can be ascribed to C-H stretching vibration from the imidazole ring and the methyl group in the linker, respectively (Nafisi and Hägg, 2014b). The peak at 1585 cm^{-1} can be attributed to the C=N stretching vibration. The peaks at 1456 cm^{-1} and 1382 cm^{-1} are related to the stretching vibration of the entire imidazole ring. The peaks in the range of 1310 – 900 cm^{-1} can be assigned to the in-plane bending of the imidazole ring. The peaks at 759 cm^{-1} and 693 cm^{-1} are related to the aromatic C-H bending. The most importantly, the presence of a strong peak at 420 indicated the Zn-N stretching in ZIF-8 (Nordin et al., 2015). For ZIF-8-PEI, in addition to the characteristic peaks of ZIF-8, the increase of the intensity of peaks at 2827 cm^{-1} and 2935 cm^{-1} corresponding to aliphatic C-H stretching vibration indicates the successful attachment of PEI polymer chains. The peak representing the hydrogen bond and the amino stretching vibration from PEI was found at 3300 cm^{-1}. Moreover, the peaks at 1458 cm^{-1} and 1585 cm^{-1} are also associated with N-H vibration of primary and secondary amino groups, respectively (Kasprzak et al., 2015). For [P(3)HIm][Tf_2N], peaks at 3158 cm^{-1}, 1579 cm^{-1}, 1452 cm^{-1}, 1347 cm^{-1} are attributed to the aromatic C-H stretching, C=N stretching, C=C stretching, and C-N stretching from [P(3)HIm] cation, respectively. Peaks at 1186 cm^{-1}, 1134 cm^{-1}, and 1055 cm^{-1} were related to the C-F stretching, S=O stretching, and S-N-S stretching from [Tf_2N] anion (Abdollahi et al., 2018). It was found that the characteristic peaks of 514 cm^{-1}, 572 cm^{-1}, 615 cm^{-1}, 654 cm^{-1}, 1055 cm^{-1}, 1186 cm^{-1}, 1452 cm^{-1}, and 1579 cm^{-1} from [P(3)HIm][Tf_2N] were present in ZIF-8-PEI@IL, indicating the successful decoration of ILs on ZIF-8. Moreover, peaks at 1452 cm^{-1} and 1579 cm^{-1} showed a blue shift in ZIF-8-PEI@IL, which indicates the strong interaction between ZIF-8 and ILs (Liu et al., 2020).

TGA measurements for the ZIF-8, ZIF-8-PEI, and ZIF-8-PEI@IL were performed in the temperature range from 25 °C to 950 °C under the nitrogen atmosphere. FTIR spectrometer was combined with TGA to analyze gas products. As it is shown in Fig. 5, there was a slight mass loss in at 100–200 °C, indicating the removal of residual molecules of H_2O, DMF, ethanol, and methanol. For ZIF-8, the main mass loss occurred at 550–900 °C due to the thermal decomposition of ZIF-8, which confirmed the high thermal stability of synthesized ZIF-8 (Zheng et al., 2019). For ZIF-8-PEI, the first main mass loss started at around 200 °C and ended at around 500 °C, which is attributed to the thermal decomposition of PEI polymer chains (K. Li et al., 2015). The second main mass loss is seen in the temperature range of 550–900 °C, which is attributed to the thermal decomposition of ZIF-8. Similar to ZIF-8-PEI, the first main mass loss (200–500 °C) of ZIF-8-PEI@IL was related to the decomposition of PEI polymer chains and ILs (Xu and Cheng, 2021), while the second mass loss (500–900 °C) indicates the decomposition of ZIF-8. As it is shown in Figs. S8 and S9, the characteristic peaks at 3000–3400 cm^{-1} could be assigned to the produced gases of NH_3, CH_4, C_2H_4, C_2H_6 and H_2O vapor. The characteristic peaks at 731–741 cm^{-1} and 2200–2400 cm^{-1} could be attributed to CO_2. The characteristic peaks at 1078 cm^{-1} and 1151–1160 cm^{-1} could be related to SO_2 and H_2S. The weak peak at 4068 cm^{-1} is related to HF. The increase of the intensity of peaks at 3000–3400 cm^{-1}, 731–741 cm^{-1}, and 2200–2400 cm^{-1} indicates the successful attachment of PEI chains on ZIF-8 since PEI mainly contains C and N (Fig. S8b). The presence of peaks at 1078 cm^{-1}, 1151–1160 cm^{-1}, and 4068 cm^{-1} indicates the successful decoration of ILs on ZIF-8 owing to the presence of F, O, and S in ILs.

3.2. *Characterization of MMMs*

FTIR spectra of pristine Pebax® 2533 membrane and MMMs containing 10 wt% of ZIF-8, ZIF-8-PEI or ZIF-8-PEI@IL were presented in Fig. S10. The pristine Pebax® 2533 membranes exhibited the characteristic peak at 1109 cm^{-1} which is ascribed to the C–O–C bond from the PEO segment of Pebax® 2533. Peaks at 3298, 1734, and 1640 cm^{-1} are assigned to the -N-H- stretching vibration, out-of-plane H-N-C=O vibration of amide, and O-C=O stretching vibration of carboxylic acid, respectively (Nafisi and Hägg, 2014b). After the addition of ZIF-8, ZIF-8-PEI or ZIF-8-PEI@IL into the Pebax® 2533 matrix, new peaks at 693, 759, 1150, 1312, 1340, and 1456 cm^{-1} which are related to the aromatic C-H bending, the in-plane bending of imidazole ring, and the stretching vibration of the entire imidazole ring of ZIF-8 were found in the FTIR spectra. Moreover, the FTIR spectra of MMMs exhibited a shift of the

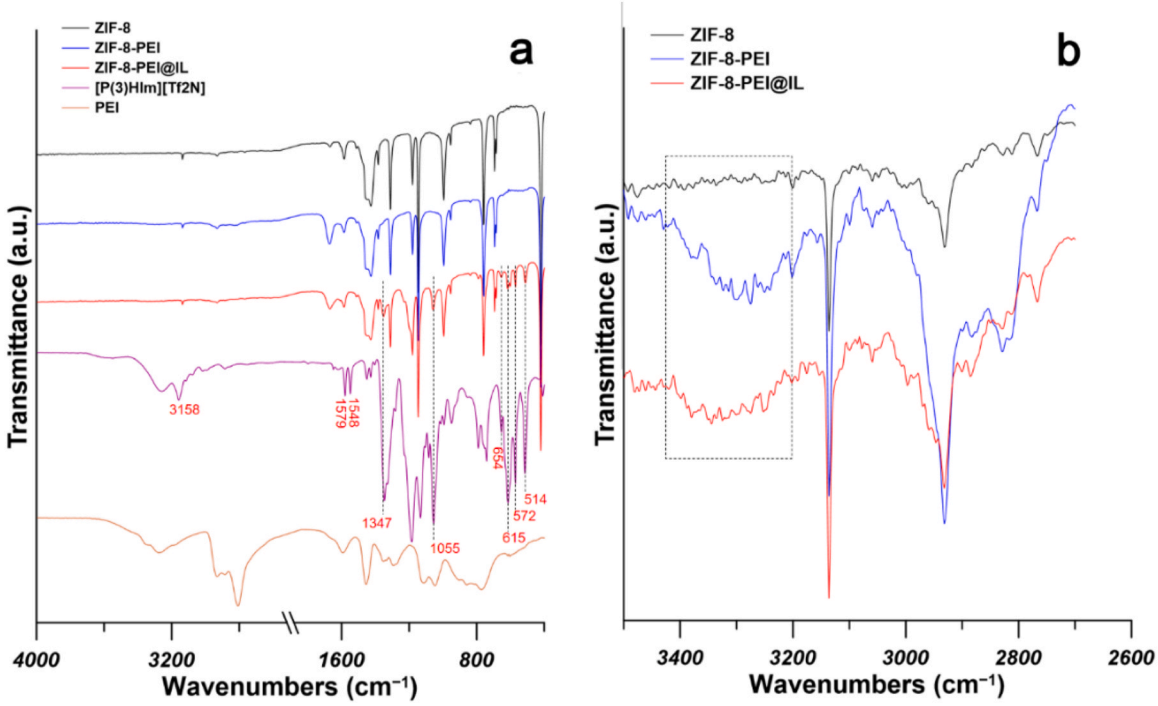

Fig. 4 – FTIR spectra of ZIF-8, ZIF-8-PEI, and ZIF-8-PEI@IL. (a) Full wavenumber range of 400–4000 cm^{-1} and (b) high wavenumber range of 2700–3600 cm^{-1}.

characteristic peaks at 3298, 1734, and 1640 cm^{-1} corresponding to the bonds of –N–H–, H–N–C=O, and O–C=O, respectively, to 3307, 1732, and 1639 cm^{-1}, respectively (Fig. S10). The shift of the characteristic peaks for Pebax® 2533 indicates the stronger molecular interactions between fillers *e.g.*, the methyl groups, amine groups, N atoms on imidazole rings from ZIF-8-PEI@IL and the polymer chains in Pebax® 2533 (Liu et al., 2021; Jiao et al., 2021). FTIR spectra of MMMs containing various amount of ZIF-8-PEI@IL were shown in Fig. S11. It was found that the intensity of characteristic peaks of ZIF-8 at 693 and 759 cm^{-1} increased with the increase of ZIF-8-PEI@IL content in MMMs.

The morphology of surface and cross-section of pristine Pebax® 2533 membrane and the prepared MMMs were investigated by SEM (Figs. 6 and 7). All the prepared membranes possess the thickness in the range of 60 – 100 µm. As it is shown in Fig. 6(a–d), the surface of pristine Pebax® 2533 membrane is smooth while the surfaces of MMMs are rough. This is because the crystallinity of the polyether and polyamide blocks decreased after the addition of fillers (Zhang et al., 2018). No defects were observed on the membrane surface. As it is shown in Fig. 6(f and j), the slight agglomeration was observed when 10 wt% ZIF-8 was incorporated into Pebax® 2533 matrix. However, there were no visible voids at the interface between ZIF-8 agglomerates and polymer, indicating the good compatibility between ZIF-8 and polymer. As it is shown in Fig. 6(g, h, k, and l), no agglomeration was observed when 10 wt% of ZIF-8-PEI or ZIF-8-PEI@IL was incorporated into Pebax® 2533 matrix, indicating the homogeneous distribution of modified ZIF-8 in polymer matrix. It was concluded that the surface modification could further improve the compatibility between ZIF-8 and polymer by

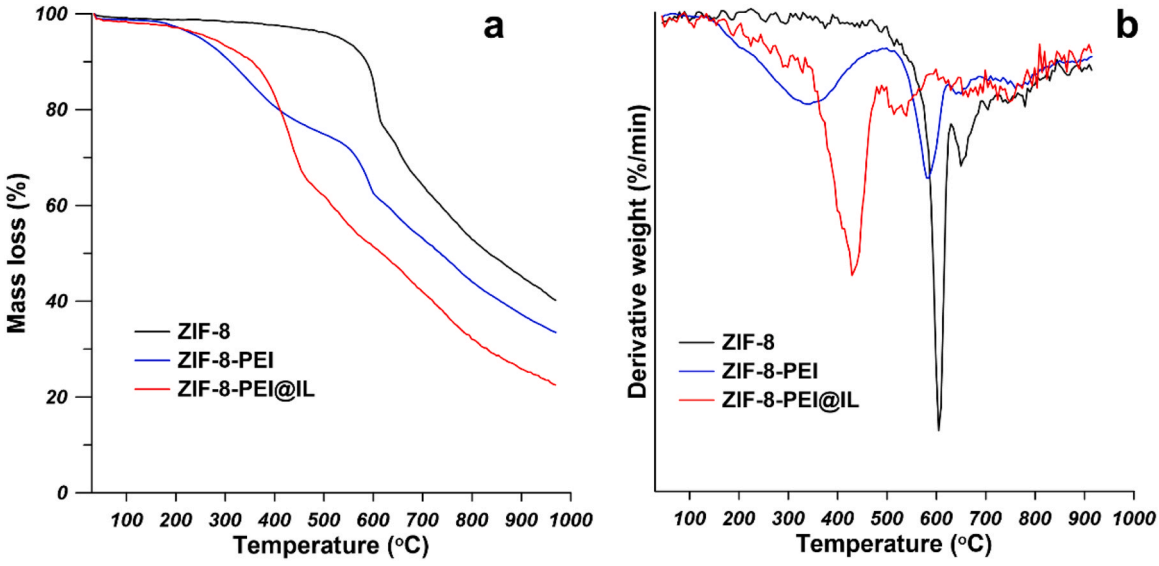

Fig. 5 – (a) TGA and (b) DTG curves of ZIF-8, ZIF-8-PEI, and ZIF-8-PEI@IL.

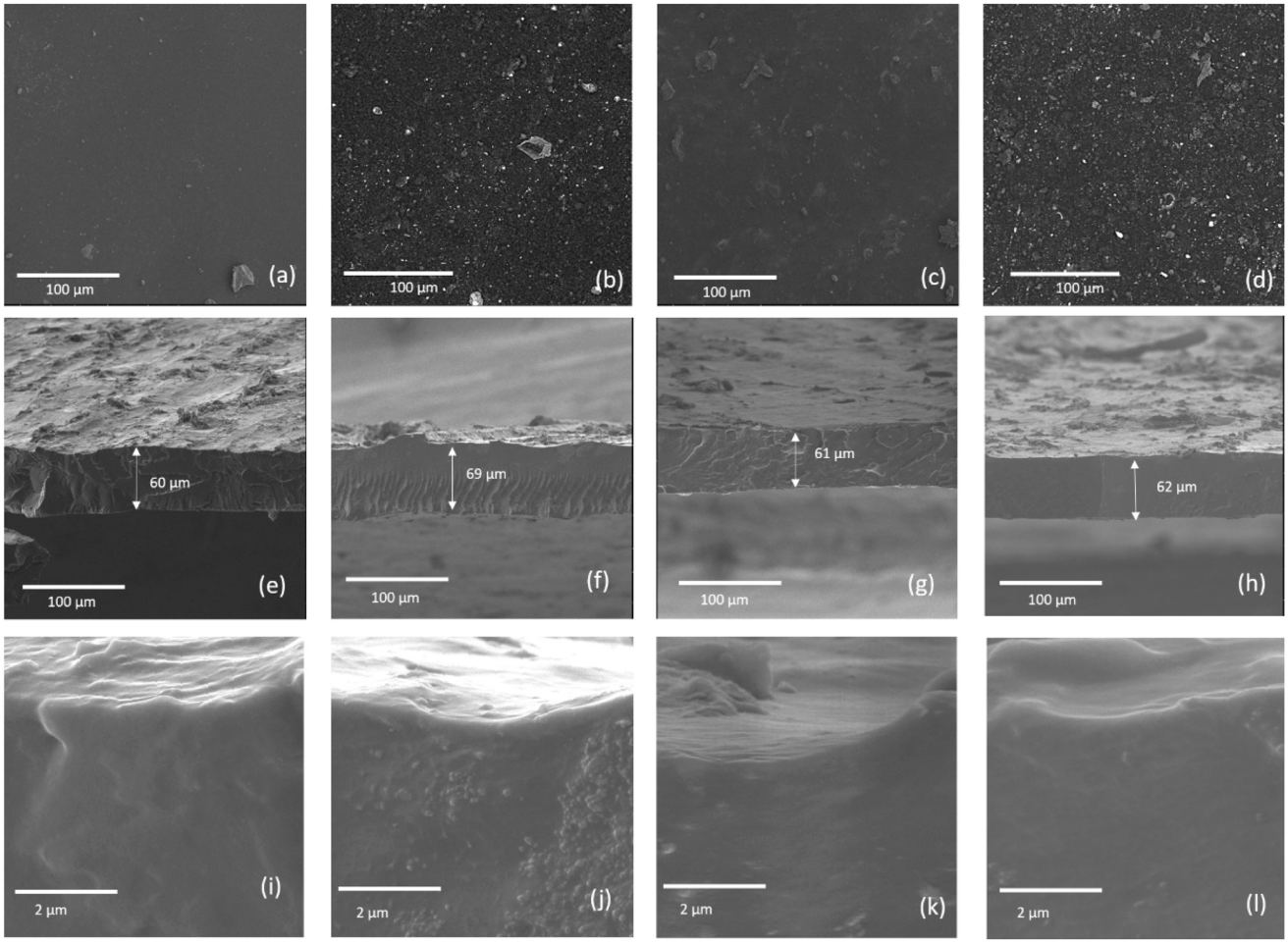

Fig. 6 – SEM images of surface (top row) and cross-section (middle and bottom rows) of the pristine Pebax® 2533 membrane (a, e, and i); MMMs with 10 wt% ZIF-8 (b, f, and j); MMMs with 10 wt% ZIF-8-PEI (c, g, and k); and MMMs with 10 wt% ZIF-8-PEI@IL (d, h, and l).

enhancing the molecular interaction, *e.g.* hydrogen bond between modified filler and polymer chains and applying ILs as sealant to inhibit the formation of interfacial voids (Li et al., 2016). Consequently, the prepared MMMs are dense and defect-free, which results in a high gas separation performance.

As shown in Fig. 7(a-e), the surfaces of MMMs became rougher with the increase of ZIF-8-PEI@IL content, which was also confirmed by AFM images (Fig. S12). As shown in Fig. 7(l–n), the ZIF-8-PEI@IL particles were dispersed homogeneously in polymer matrix at low filler content. No large agglomerates and interfacial voids were observed. However, the mild agglomeration of ZIF-8-PEI@IL particles was found in MMMs with 20 wt% loading. Nevertheless, no interfacial voids were observed in the prepared MMMs.

The thermal stability of pristine Pebax® 2533 membrane, MMMs containing different types of fillers and MMMs containing different amount of ZIF-8-PEI@IL was evaluated (Fig. S13). It was found that the thermal stability of Pebax® 2533 membrane was barely influenced after the incorporation of nanofillers. All the prepared membranes were thermally stable up to 300 °C which is far higher than the experimental temperatures (24, 35, 40, and 45 °C). The thermal decomposition of the polymer chains occurred at 420 °C. The decomposition of PEI chains and ILs occurred at 340 °C (Fig. S13).

The elongation at break and tensile strength were determined to investigate the effect of the prepared nanofillers on the mechanical properties of MMMs. As it is shown in Fig. 8, all the prepared membranes are flexible due to their high elongation at break with sufficient mechanical resistance for gas permeance tests. The pristine Pebax® 2533 membranes showed the tensile strength equal to 9.6 MPa and the elongation at break equal to 840%. The mechanical strength of the Pebax membranes was mainly determined by the rigid hydrophobic PA parts, while the elongation at break was mainly determined by the soft PE parts (Li et al., 2016). The MMMs containing 10 wt% of ZIF-8, ZIF-8-PEI, and ZIF-8-PEI@IL showed the tensile strength equal to 10.1 MPa, 10.6 MPa, and 10.2 MPa, respectively, whereas the elongation at break was equal to 780%, 996%, and 960%, respectively (Fig. 8a). In comparison to the pristine Pebax® 2533 membranes and MMMs containing ZIF-8, MMMs containing ZIF-8-PEI, and ZIF-8-PEI@IL exhibited higher tensile strength and elongation at break, which indicates the good dispersion and improved compatibility of modified ZIF-8 owing to the formation of hydrogen bonds between the modified ZIF-8 and the polymer matrix. Therefore, the interaction force between the modified ZIF-8 and polymer chains increased resulting in the improved mechanical properties of MMMs (Liu et al., 2021). As it is shown in Fig. 8b, both the elongation at break and the tensile strength increased with the increase of ZIF-8-PEI@IL

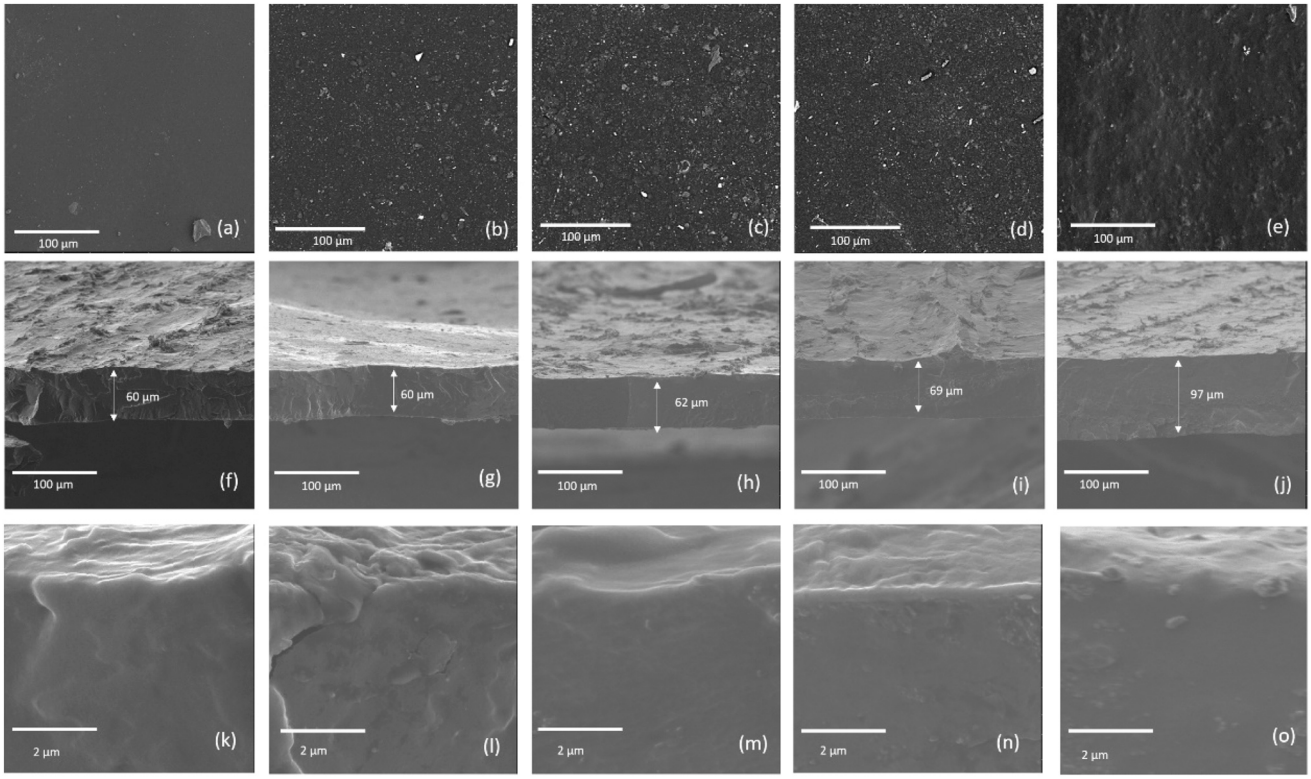

Fig. 7 – SEM images of surface (top row) and cross-section (middle and bottom rows) of the pristine Pebax® 2533 membrane (a, f, and k); MMMs with 5 wt% (b, g, and l), 10 wt% (c, h, and m), 15 wt% (d, I, and n), and 20 wt% (e, j, and o) of ZIF-8-PEI@IL.

up to 15 wt%. The further increase of filler content to 20 wt% resulted in the significant decrease of the elongation at break (45%) and the tensile strength (24%), in comparison to pristine Pebax® 2533 membranes. This is because the nanofiller agglomeration occurred at higher nanofiller content as it is shown in the SEM images (Fig. 7). The interface between nanofillers and polymer matrix became rigidified due to the agglomeration of nanofillers, resulting in the decrease of crystallinity of MMMs (Liu et al., 2021; Behroozi and Pakizeh, 2017).

3.3. *Gas permeation measurements of MMMs*

3.3.1. *The effect of filler type on gas permeability and ideal selectivity*

The pure gas permeability and the ideal selectivity of CO_2/N_2, CO_2/CH_4, and CO_2/H_2 of pristine Pebax® 2533 membranes and MMMs containing 10 wt% of ZIF-8, ZIF-8-PEI, or ZIF-8-PEI@IL were presented in Fig. 9. All the prepared MMMs showed higher CO_2 permeability and ideal selectivity than the pristine Pebax® 2533 membrane. Therefore, the incorporation of

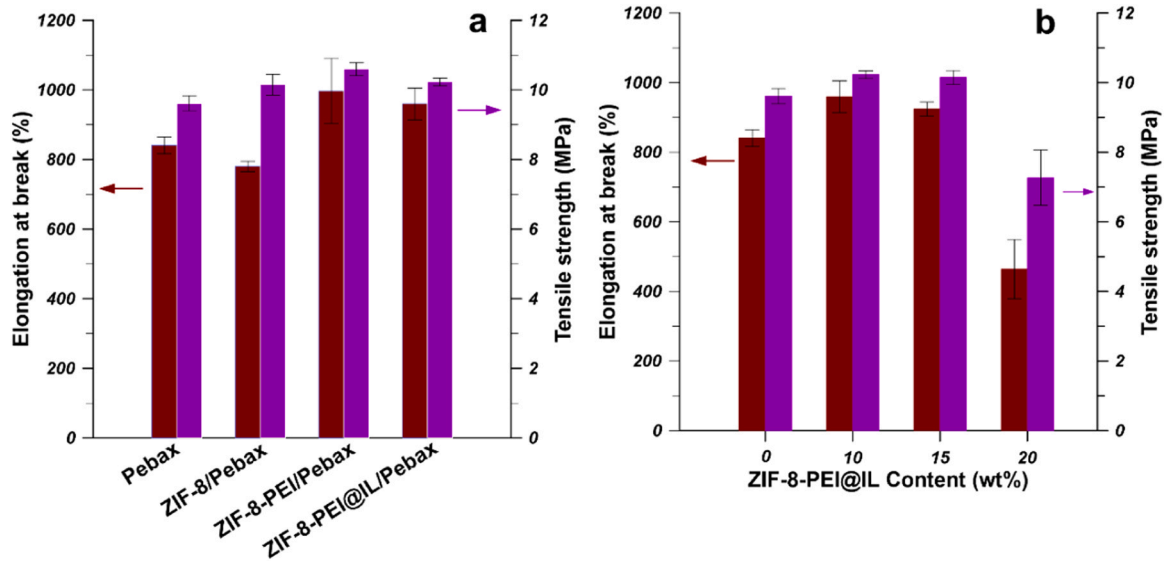

Fig. 8 – Mechanical properties of (a) pristine Pebax® 2533 membranes and MMMs containing 10 wt% of ZIF-8, ZIF-8-PEI, and ZIF-8-PEI@IL, and (b) MMMs containing different amount of ZIF-8-PEI@IL.

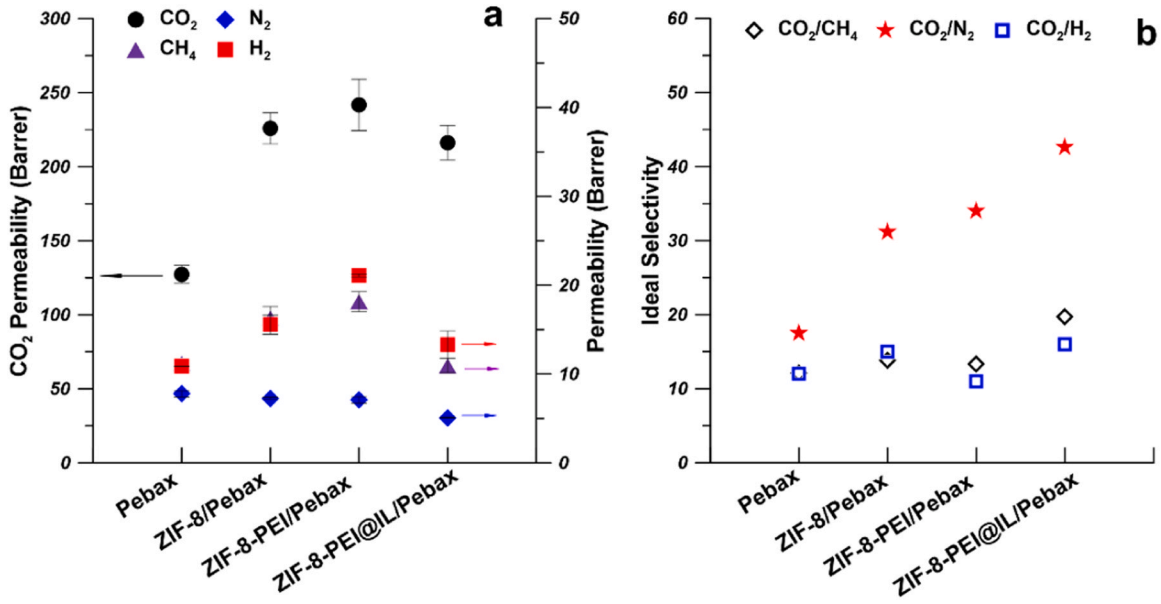

Fig. 9 – (a) Gas permeability and (b) ideal selectivity of MMMs containing various types of fillers (filler content 10 wt%, experimental condition: 24 °C and 2 bar).

pristine and modified ZIF-8 could improve the gas separation performance of membranes. In the pristine Pebax® 2533 membrane, it was found that the H_2 permeability is lower than the CO_2 permeability even though the kinetic diameter of H_2 (0.29 nm) is smaller than CO_2 (0.33 nm). This is because PEO chains show strong dipole-quadrupole interactions with polar gases such as CO_2. Moreover, CO_2 possesses high condensability. Therefore, the gas permeability is mainly determined by gas solubility in Pebax® 2533 (Bernardo and Clarizia, 2020). After the incorporation of porous pristine and modified ZIF-8, CO_2 permeability was significantly enhanced due to the smaller kinetic diameter than the ZIF-8 aperture (0.34 nm) and the strong interaction between filler and CO_2 molecules (Liu et al., 2021). H_2 permeability was higher than that of pristine Pebax® 2533 membrane owing to the smaller kinetic diameter and transporting path provided by ZIF-8. Even though the kinetic diameter of CH_4 (0.38 nm) is higher than that of N_2 (0.36 nm), CH_4 permeability is higher that N_2 permeability. This is because the solubility coefficient of CH_4 is higher than that of N_2 when the ZIF-8 was incorporated into Pebax® 2533 (Li et al., 2017). N_2 permeability is the lowest because N_2 possesses lowest solubility coefficient and bigger kinetic diameter than the ZIF-8 aperture (Li et al., 2017). As a result, the CO_2/N_2 selectivity increased much more significantly than CO_2/CH_4 and CO_2/H_2 selectivity.

Among these three types of porous fillers, ZIF-8-PEI@IL showed the most desirable effect on the CO_2 separation performance of MMMs. MMMs containing ZIF-8-PEI@IL exhibited the highest selectivity of CO_2/N_2, CO_2/CH_4 and CO_2/H_2 which are equal to 43, 20 and 16, respectively and high CO_2 permeability equal to 216 Barrer (Fig. 9). The high CO_2 permeability of MMMs containing ZIF-8-PEI@IL was resulted from the presence of ZIF-8-PEI@IL pores, the additional facilitated transport path for CO_2 molecules, the enhanced interfacial compatibility between fillers and Pebax® 2533 polymer chains, and the enhanced CO_2 affinity to fillers by ILs (Jiao et al., 2021). Specifically, the pores from fillers provide additional paths for such gas molecules as CO_2. The presence of PEI containing plenty of primary and secondary amino groups as CO_2 carriers endows the MMMs with facilitated transport mechanism for CO_2 molecules (Y. Li et al., 2015). The reversible reactions between primary and secondary amino groups and CO_2 molecules are shown by Eqs. (3) and (4) (Li et al., 2015):

$$CO_2 + RR'NH \rightleftharpoons RR'NH^+COO^- \quad (3)$$

$$RR'NH^+COO^- + RR'NH \rightleftharpoons RR'NCOO^- + RR'NH_2^+ \quad (4)$$

where R′ is hydrogen atom or other organic groups. Moreover, the amino groups improved the interfacial compatibility *via* the interaction with Pebax® 2533 chains, such as the interaction between -NH_2 and C═O in the PA segment and the interaction between N-H and C-O in the PEO segment of Pebax® 2533 (Jiao et al., 2021). CO_2 exhibited high solubility in ILs ([P(3)HIm][Tf_2N]) (Zoubeik et al., 2016). Therefore, the ILs decoration improved the CO_2 affinity of ZIF-8, which is beneficial to the increase of CO_2 permeability of MMMs. What is also important, ILs could be used as sealants between fillers and polymer chains to enhance their compatibility (Li et al., 2016).

MMMs containing ZIF-8-PEI@IL exhibited the highest ideal selectivity owing to the high CO_2 permeability and lower permeability of N_2, CH_4, and H_2, comparing with MMMs containing ZIF-8 or ZIF-8-PEI. On one hand, the low permeability of big gas molecular (N_2, and CH_4) was related to the reduced pore volume and aperture size of modified ZIF-8, which decreased the gas adsorption capacity of fillers. Consequently, the molecular sieving properties of MMMs were enhanced (Li et al., 2016). The permeability of hydrogen is low because hydrogen is non-polar gas which shows low solubility coefficient in the Pebax® 2533 based MMMs (Jansen et al., 2013). On the other hand, the incorporation of ZIF-8-PEI@IL into Pebax® 2533 matrix significantly increased the CO_2 permeability. Therefore, MMMs containing ZIF-8-PEI@IL exhibited the highest ideal selectivity. According to the above discussion, the probable pathways of gas molecules (CO_2, N_2, and CH_4) are visualized in Fig. S14.

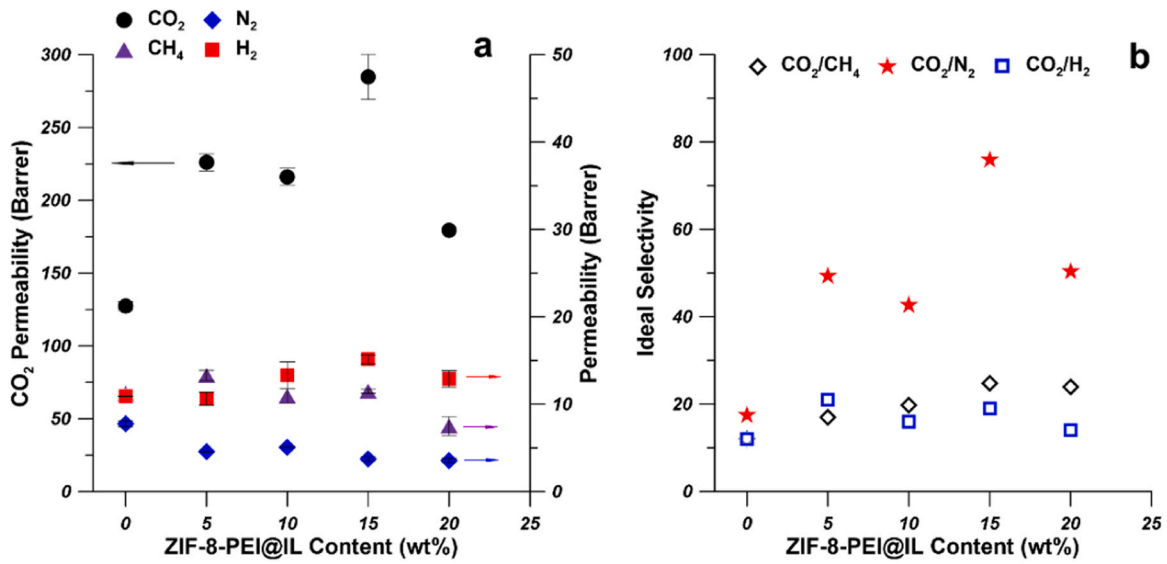

Fig. 10 – (a) Gas permeability and (b) ideal selectivity of MMMs containing various amount of ZIF-8-PEI@IL (experimental condition: 24 °C and 2 bar).

3.3.2. The effect of filler content on gas permeability and ideal selectivity

MMMs containing ZIF-8-PEI@IL showed the best gas separation performance considering the permeability and selectivity. Therefore, the effects of amount of ZIF-8-PEI@IL on the gas permeability and selectivity of MMMs have been investigated. As it is shown in Fig. 10a, in comparison to pristine Pebax® 2533 membrane, CO_2 permeability significantly increased when ZIF-8-PEI@IL was incorporated. Moreover, CO_2 permeability increased to a peak value of 285 Barrer with the increase of filler content to 15 wt% owing to the gas molecule transport path provided by porous ZIF-8-PEI@IL, the additional facilitated transport path for CO_2 molecules, and the enhanced CO_2 affinity to fillers by ILs (Jiao et al., 2021). The further increase of ZIF-8-PEI@IL resulted in the decrease of CO_2 permeability which can be related to the agglomeration of fillers which might hinder at the center of polymer chains and block the passage of the gas molecules (Liu et al., 2021). Similar relationship between CO_2 permeability and filler content in MMMs was reported by Jiao et al. (2021). In their research, as PEI-ZIF-8 content increased in Pebax® 2533 matrix, CO_2 permeance and selectivity firstly increased and subsequently decreased. It was suggested that the decline in CO_2 permeance resulted from the over-loading of PEI-ZIF-8 fillers which produced rigidified interface (Jiao et al., 2021).

The gas permeability of CH_4 and N_2 decreased slightly while the H_2 permeability increased slightly with the increase of filler content in MMMs due to the size sieving effect (Li et al., 2016). The permeabilities of CH_4, N_2, and H_2 were changed slightly because they are non-polar gas molecules possessing low solubility coefficient in Pebax® 2533-based MMMs (He et al., 2021; Zhao et al., 2014). According to the solution diffusion mechanism, the gas permeability through Pebax® 2533-based MMMs is mainly determined by solubility coefficient rather than the diffusion coefficient (Li et al., 2021b). Consequently, the selectivity of CO_2/N_2 and CO_2/CH_4 increased with the increase of filler content in MMMs (Fig. 10b). At 15 wt% of ZIF-8-PEI@IL, MMMs exhibited the highest gas selectivity equal to 76 and 25 for CO_2/N_2 and CO_2/CH_4, respectively. It was found that the incorporation of ZIF-8-PEI@IL did not increase the CO_2/H_2 selectivity significantly, indicating the effect of ZIF-8 fillers on CO_2/H_2 separation performance of Pebax® 2533 based MMMs is limited owing to the nature of Pebax® 2533 polymer matrix.

3.3.3. The effect of temperature on gas permeability and ideal selectivity

The gas permeability and selectivity at various temperatures (24, 35, 40, and 45 °C) were tested to investigate the effect of temperature on the gas separation performance of pristine Pebax® 2533 membranes and the prepared MMMs containing ZIF-8-PEI@IL. As it is shown in Fig. 11, with an increase of temperature, gas (CO_2, N_2, CH_4 and H_2) permeability of pristine Pebax® 2533 membranes and prepared MMMs increased, while the selectivity of all membranes exhibited a decreasing trend. The decline of gas selectivity of membranes with increasing temperature can be explained in the following way. On one hand, the movement of polymer chains was enhanced at higher temperature, leading to the increase of the free volume and the formation of less selective membranes allowing bigger molecules to permeate through membranes (Gou et al., 2021). On the other hand, the increment of diffusion rate of molecules with smaller molecular weight was more significant than for molecules with bigger molecular weight, while the solubility coefficient of gas molecules in membrane decreased at higher temperature (Gülmüs and Yilmaz, 2007). Therefore, the gas selectivity decreased with the increase of temperature.

Additionally, the effect of temperature on gas permeability can be estimated by using the Arrhenius Eq. (5) (Bernardo and Clarizia, 2020):

$$P_i = P_{i,0}\exp\left(\frac{-E_p}{RT}\right) \quad (5)$$

where P_i is the permeability of component i, $P_{i,0}$ is pre-exponential factor, E_p is the activation energy, R is the gas constant, and T is the operation temperature in Kelvin. It was found that the E_p values of all tested gases in the prepared MMMs were higher than the those in pristine Pebax® 2533 membranes (Table S2), indicating the change of the energy barrier of gas permeation through membranes resulted from the incorporation of ZIF-8-PEI@IL (Sun et al., 2019). The E_p value of CO_2 in both the pristine Pebax® 2533 membrane and MMMs is the lowest, which suggests the lower activation

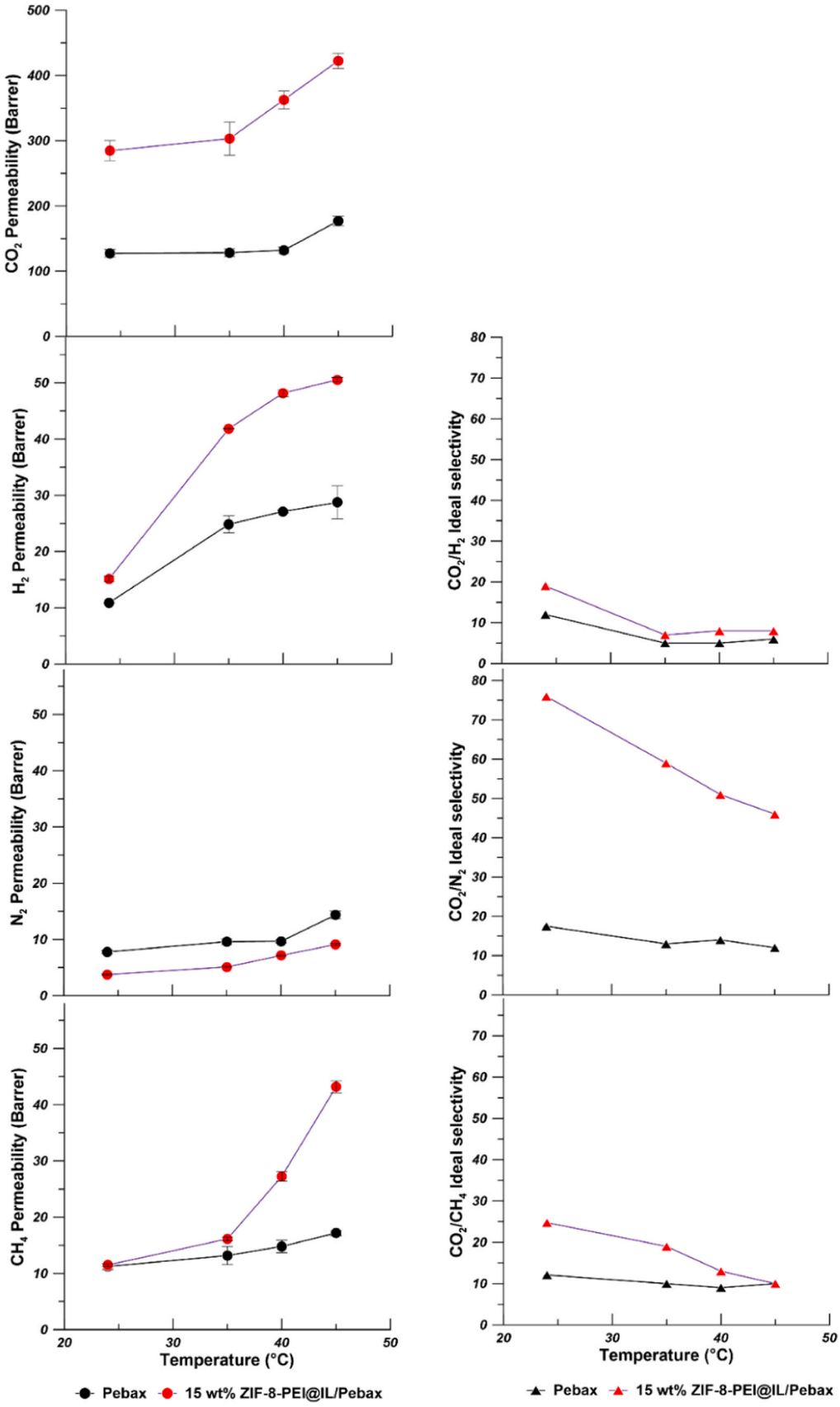

Fig. 11 – Gas permeability and selectivity of pristine Pebax® 2533 membrane and MMMs containing 15 wt% of ZIF-8-PEI@IL at various temperatures.

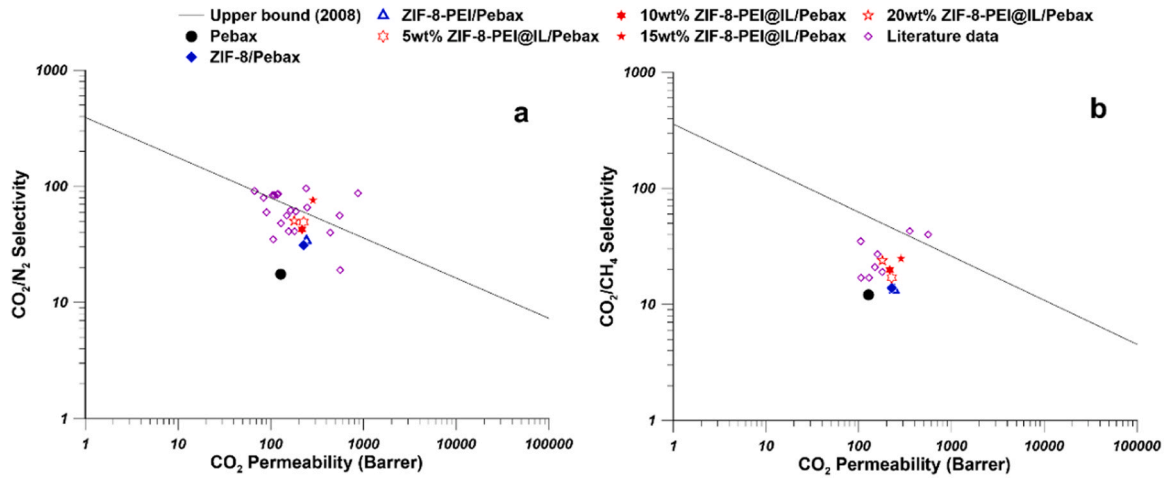

Fig. 12 – The comparison of the performance of MMMs with Robeson upper bound (2008) for (a) CO_2/N_2 and (b) CO_2/CH_4 (the gas permeability and selectivity in this work were obtained by using pure gas testing; the literature data were taken from Table S3).

energy of CO_2 permeating through the membranes. The obtained results are consistent with the previous reports which revealed that larger gas molecules exhibited higher activation energy of permeation through membranes (Stevens et al., 2020). The orders of E_p were $N_2 > CH_4 > H_2 > CO_2$ and $CH_4 > N_2 > H_2 > CO_2$ for pristine Pebax® 2533 membrane and prepared MMMs, respectively (Table S2). The high values of activation energy of permeation for N_2 and CH_4 indicate that the permeability of these bigger and less permeable gases were strongly affected by temperature change (Lasseuguette et al., 2018). CO_2 possessed the lowest E_p and superior solubility in Pebax® 2533 membrane and prepared MMMs. With the increase of temperature, gas solubility decreased, while CO_2 permeability is mainly dominated by solubility in Pebax® 2533 based membranes (Lasseuguette et al., 2018). Therefore, the CO_2 permeability was less influenced by the increase of temperature than N_2 and CH_4, resulting in the decline of CO_2/N_2 and CO_2/CH_4 selectivity.

3.3.4. *The comparison with literature data of MMMs*

The gas permeability and selectivity of prepared MMMs were compared with the Robeson's upper bound (Robeson, 2008). As it is shown in Fig. 12, ZIF-8-PEI@IL/Pebax® 2533 MMMs exhibited much higher permselectivity than pristine Pebax® 2533 membranes for CO_2/N_2 and CO_2/CH_4 separations. The CO_2/N_2 separation performance of prepared ZIF-8-PEI@IL/Pebax® 2533 MMMs surpassed the Robeson's upper bound (2008). While the CO_2/CH_4 separation performance of prepared ZIF-8-PEI@IL/Pebax® 2533 MMMs is approaching the Robeson's upper bound (2008). MMMs containing 15 wt% ZIF-8-PEI@IL showed the best gas separation performance for CO_2/N_2 and CO_2/CH_4 separations. The prepared MMMs containing 15 wt% ZIF-8-PEI@IL showed high CO_2 permeability equal to 285 Barrer along with CO_2/N_2 selectivity of 76 and CO_2/CH_4 selectivity of 25. As it is shown in Table S3 and Fig. 12, the performance of MMMs containing 15 wt% ZIF-8-PEI@IL is comparable with reported performances of Pebax based MMMs. Consequently, the modification of ZIF-8 with PEI along with the decoration of ILs is an encouraging way to improve the gas separation performance of MMMs *via* the additional gas molecules transport pathways, improved filler affinity to CO_2 and enhancement of compatibility between filler and polymer matrix.

4. Conclusions

ZIF-8-PEI@[P(3)HIm][Tf_2N] composite fillers were designed and prepared for the successful fabrication of Pebax® 2533-based MMMs for CO_2 separation. The crystal structure of ZIF-8 was preserved, while the BET surface area, total pore volume, and average pore diameter decreased after modification due to the presence of PEI and ILs in ZIF-8. It was found that the compatibility between filler and polymer matrix was significantly enhanced owing to the enhanced molecular interactions between amino groups in PEI and Pebax polymer chains. Moreover, the decoration of ILs on ZIF-8-PEI further optimized the interfacial morphology of MMMs by inhibiting the formation of interfacial voids. As a result, the mechanical properties of MMMs were enhanced, confirmed by the increased elongation at break and tensile strength. In comparison to the pristine Pebax® 2533 membranes, the ZIF-8-PEI@IL/Pebax® 2533 MMMs exhibited significant improvement of gas separation performance due to the size sieving effect of ZIF-8-PEI@IL, the additional facilitated CO_2 molecules transport path from amino groups on PEI, and the enhanced CO_2 affinity to fillers by ILs. CO_2 permeability of MMMs containing 15 wt% ZIF-8-PEI@IL increased 123% to 285 Barrer, and the CO_2/N_2 and CO_2/CH_4 ideal selectivity increased from 17 and 12 to 76 and 25, respectively.

Declaration of Competing Interest

The authors declare that they have no known competing financial interests or personal relationships that could have appeared to influence the work reported in this paper.

Acknowledgements

This work was supported by the PROM project, funded by Polish National Agency for Academic Exchange NAWA (agreement no.: PPI/PRO/2019/1/00015/U/00001)

Appendix A. Supplementary material

Supplementary data associated with this article can be found in the online version at doi:10.1016/j.cherd.2022.03.023.

References

Abdollahi, S., Mortaheb, H.R., Ghadimi, A., Esmaeili, M., 2018. Improvement in separation performance of Matrimid®5218 with encapsulated [Emim][Tf2N] in a heterogeneous structure: CO_2/CH_4 separation. J. Membr. Sci. 557, 38–48.

Abd, A.A., Othman, M.R., Naji, S.Z., Hashim, A.S., 2021. Methane enrichment in biogas mixture using pressure swing adsorption: process fundamental and design parameters. Mater. Today Sustain. 11–12, 100063.

ALOthman, Z.A., 2012. A review: fundamental aspects of silicate mesoporous materials. Materials 5, 2874–2902.

Anderson, W., Kozak, D., Coleman, V.A., Jämting, Å.K., Trau, M., 2013. A comparative study of submicron particle sizing platforms: accuracy, precision and resolution analysis of polydisperse particle size distributions. J. Colloid Interface Sci. 405, 322–330.

Atash Jameh, A., Mohammadi, T., Bakhtiari, O., 2020. Preparation of PEBAX-1074/modified ZIF-8 nanoparticles mixed matrix membranes for CO_2 removal from natural gas. Sep. Purif. Technol. 231, 115900.

Behroozi, M., Pakizeh, M., 2017. Study the effects of Cloisite15A nanoclay incorporation on the morphology and gas permeation properties of Pebax2533 polymer. J. Appl. Polym. Sci. 134, 45302.

Bernardo, P., Clarizia, G., 2020. Enhancing gas permeation properties of Pebax® 1657 membranes via polysorbate nonionic surfactants doping. Polymers 12, 253.

Chi, W.S., Hwang, S., Lee, S.-J., Park, S., Bae, Y.-S., Ryu, D.Y., Kim, J.H., Kim, J., 2015. Mixed matrix membranes consisting of SEBS block copolymers and size-controlled ZIF-8 nanoparticles for CO_2 capture. J. Membr. Sci. 495, 479–488.

Cui, L., Liu, M., Yuan, X., Wang, Q., Ma, Q., Wang, P., Hong, J., Liu, H., 2021. Environmental and economic impact assessment of three sintering flue gas treatment technologies in the iron and steel industry. J. Clean. Prod. 311, 127703.

Dal-Cin, M.M., Kumar, A., Layton, L., 2008. Revisiting the experimental and theoretical upper bounds of light pure gas selectivity–permeability for polymeric membranes. J. Membr. Sci. 323, 299–308.

Ding, R., Zheng, W., Yang, K., Dai, Y., Ruan, X., Yan, X., He, G., 2020. Amino-functional ZIF-8 nanocrystals by microemulsion based mixed linker strategy and the enhanced CO_2/N_2 separation. Sep. Purif. Technol. 236, 116209.

Gao, J., Mao, H., Jin, H., Chen, C., Feldhoff, A., Li, Y., 2020. Functionalized ZIF-7/Pebax® 2533 mixed matrix membranes for CO_2/N_2 separation. Microporous Mesoporous Mater. 297, 110030.

Gouveia, A.S.L., Yáñez, M., Alves, V.D., Palomar, J., Moya, C., Gorri, D., Tomé, L.C., Marrucho, I.M., 2021. CO_2/H_2 separation through poly(ionic liquid)–ionic liquid membranes: the effect of multicomponent gas mixtures, temperature and gas feed pressure. Sep. Purif. Technol. 259, 118113.

Gou, M., Zhu, W., Sun, Y., Guo, R., 2021. Introducing two-dimensional metal-organic frameworks with axial coordination anion into Pebax for CO_2/CH_4 separation. Sep. Purif. Technol. 259, 118107.

Gülmüs, S.A., Yilmaz, L., 2007. Effect of temperature and membrane preparation parameters on gas permeation properties of polymethacrylates. J. Polym. Sci. Part B Polym. Phys. 45, 3025–3033.

Hao, L., Li, P., Yang, T., Chung, T.-S., 2013. Room temperature ionic liquid/ZIF-8 mixed-matrix membranes for natural gas sweetening and post-combustion CO_2 capture. J. Membr. Sci. 436, 221–231.

He, R., Cong, S., Xu, S., Han, S., Guo, H., Liang, Z., Wang, J., Zhang, Y., 2021. CO_2-philic mixed matrix membranes based on low-molecular-weight polyethylene glycol and porous organic polymers. J. Membr. Sci. 624, 119081.

He, S., Zhu, B., Li, S., Zhang, Y., Jiang, X., Hon Lau, C., Shao, L., 2022. Recent progress in PIM-1 based membranes for sustainable CO_2 separations: polymer structure manipulation and mixed matrix membrane design. Sep. Purif. Technol. 284, 120277.

Inoue, M., Hirasawa, I., 2013. The relationship between crystal morphology and XRD peak intensity on $CaSO_4{\cdot}2H_2O$. J. Cryst. Growth 380, 169–175.

Jansen, J.C., Clarizia, G., Bernardo, P., Bazzarelli, F., Friess, K., Randová, A., Schauer, J., Kubicka, D., Kacirková, M., Izak, P., 2013. Gas transport properties and pervaporation performance of fluoropolymer gel membranes based on pure and mixed ionic liquids. Sep. Purif. Technol. 109, 87–97.

Jiao, C., Li, Z., Li, X., Wu, M., Jiang, H., 2021. Improved CO_2/N_2 separation performance of Pebax composite membrane containing polyethyleneimine functionalized ZIF-8. Sep. Purif. Technol. 259, 118190.

Ji, L., Zhang, L., Zheng, X., Feng, L., He, Q., Wei, Y., Yan, S., 2021. Simultaneous CO_2 absorption, mineralisation and carbonate crystallisation promoted by amines in a single process. J. CO2 Util. 51, 101653.

Kamble, A.R., Patel, C.M., Murthy, Z.V.P., 2021. A review on the recent advances in mixed matrix membranes for gas separation processes. Renew. Sustain. Energy Rev. 145, 111062.

Kasprzak, A., Popławska, M., Bystrzejewski, M., Łabędź, O., Grudziński, I.P., 2015. Conjugation of polyethylenimine and its derivatives to carbon-encapsulated iron nanoparticles. RSC Adv. 5, 85556–85567.

Kim, S.Y., Cho, Y., Kang, S.W., 2020. Correlation between functional group and formation of nanoparticles in PEBAX/Ag salt/al salt complexes for olefin separation. Polymers 12, 667.

Kujawski, W., Li, G., Van der Bruggen, B., Pedišius, N., Tonkonogij, J., Tonkonogovas, A., Stankevičius, A., Šereika, J., Jullok, N., Kujawa, J., 2020. Preparation and characterization of polyphenylsulfone (PPSU) membranes for biogas upgrading. Materials 13, 2847.

Lasseuguette, E., Malpass-Evans, R., Carta, M., McKeown, N.B., Ferrari, M.-C., 2018. Temperature and pressure dependence of gas permeation in a microporous Tröger's base polymer. Membranes 8, 132.

Leofanti, G., Padovan, M., Tozzola, G., Venturelli, B., 1998. Surface area and pore texture of catalysts. Catal. Today 41, 207–219.

Liu, N., Cheng, J., Hou, W., Yang, X., Zhou, J., 2021. Pebax-based mixed matrix membranes loaded with graphene oxide/core shell ZIF-8@ ZIF-67 nanocomposites improved CO_2 permeability and selectivity. J. Appl. Polym. Sci. 138, 50553.

Liu, B., Li, D., Yao, J., Sun, H., 2020. Improved CO_2 separation performance and interfacial affinity of mixed matrix membrane by incorporating UiO-66-PEI@[bmim][Tf2N] particles. Sep. Purif. Technol. 239, 116519.

Li, K., Jiang, J., Tian, S., Yan, F., Chen, X., 2015. Polyethyleneimine–nano silica composites: a low-cost and promising adsorbent for CO_2 capture. J. Mater. Chem. A 3, 2166–2175.

Li, Y., Wang, S., He, G., Wu, H., Pan, F., Jiang, Z., 2015. Facilitated transport of small molecules and ions for energy-efficient membranes. Chem. Soc. Rev. 44, 103–118.

Li, G., Kujawski, W., Knozowska, K., Kujawa, J., 2021a. Thin film mixed matrix hollow fiber membrane fabricated by incorporation of amine functionalized metal-organic framework for CO_2/N_2 separation. Materials 14, 3366.

Li, G., Kujawski, W., Válek, R., Koter, S., 2021b. A review - the development of hollow fibre membranes for gas separation processes. Int. J. Greenh. Gas Control 104, 103195.

Li, H., Tuo, L., Yang, K., Jeong, H.-K., Dai, Y., He, G., Zhao, W., 2016. Simultaneous enhancement of mechanical properties and CO_2 selectivity of ZIF-8 mixed matrix membranes: interfacial toughening effect of ionic liquid. J. Membr. Sci. 511, 130–142.

Li, M., Zhang, X., Zeng, S., bai, L., Gao, H., Deng, J., Yang, Q., Zhang, S., 2017. Pebax-based composite membranes with high gas transport properties enhanced by ionic liquids for CO_2 separation. RSC Adv. 7, 6422–6431.

Lv, X., Huang, L., Ding, S., Wang, J., Li, L., Liang, C., Li, X., 2021. Mixed matrix membranes comprising dual-facilitated bio-inspired filler for enhancing CO_2 separation. Sep. Purif. Technol. 276, 119347.

Menezes, T., Santos, K., Franceschi, E., Borges, G., Dariva, C., Egues, S., De Conto, J., Santana, C., 2020. Synthesis of the chiral stationary phase based on functionalized ZIF-8 with amylose carbamate. J. Mater. Res. 35, 2936–2949.
Nafisi, V., Hägg, M.-B., 2014a. Gas separation properties of ZIF-8/6FDA-durene diamine mixed matrix membrane. Sep. Purif. Technol. 128, 31–38.
Nafisi, V., Hägg, M.-B., 2014b. Development of dual layer of ZIF-8/PEBAX-2533 mixed matrix membrane for CO_2 capture. J. Membr. Sci. 459, 244–255.
Nath, D., Henni, A., 2020. Solubility of carbon dioxide (CO_2) in four bis (trifluoromethyl-sulfonyl)imide ([Tf2N]) based ionic liquids. Fluid Phase Equilibria 524, 112757.
Nordin, N.A.H.M., Racha, S.M., Matsuura, T., Misdan, N., Abdullah Sani, N.A., Ismail, A.F., Mustafa, A., 2015. Facile modification of ZIF-8 mixed matrix membrane for CO_2/CH_4 separation: synthesis and preparation. RSC Adv. 5, 43110–43120.
Robeson, L.M., 2008. The upper bound revisited. J. Membr. Sci. 320, 390–400.
Rynkowska, E., Fatyeyeva, K., Kujawski, W., 2018. Application of polymer-based membranes containing ionic liquids in membrane separation processes: a critical review. Rev. Chem. Eng. 34, 341–363.
Shah Buddin, M.M.H., Ahmad, A.L., 2021. A review on metal-organic frameworks as filler in mixed matrix membrane: Recent strategies to surpass upper bound for CO_2 separation. J. CO2 Util. 51, 101616.
Singh, S., Varghese, A.M., Reinalda, D., Karanikolos, G.N., 2021. Graphene-based membranes for carbon dioxide separation. J. CO2 Util. 49, 101544.
Song, Y., He, M., Zhao, J., Jin, W., 2021. Structural manipulation of ZIF-8-based membranes for high-efficiency molecular separation. Sep. Purif. Technol. 270, 118722.
Stevens, K.A., Moon, J.D., Borjigin, H., Liu, R., Joseph, R.M., Riffle, J.S., Freeman, B.D., 2020. Influence of temperature on gas transport properties of tetraaminodiphenylsulfone (TADPS) based polybenzimidazoles. J. Membr. Sci. 593, 117427.
Sun, J., Li, Q., Chen, G., Duan, J., Liu, G., Jin, W., 2019. MOF-801 incorporated PEBA mixed-matrix composite membranes for CO_2 capture. Sep. Purif. Technol. 217, 229–239.
Wee, L.H., Lescouet, T., Ethiraj, J., Bonino, F., Vidruk, R., Garrier, E., Packet, D., Bordiga, S., Farrusseng, D., Herskowitz, M., 2013. Hierarchical zeolitic imidazolate framework-8 catalyst for monoglyceride synthesis. ChemCatChem 5, 3562–3566.
Wu, D., Zhang, P.-F., Yang, G.-P., Hou, L., Zhang, W.-Y., Han, Y.-F., Liu, P., Wang, Y.-Y., 2021. Supramolecular control of MOF pore properties for the tailored guest adsorption/separation applications. Coord. Chem. Rev. 434, 213709.
Xian, S., Xu, F., Ma, C., Wu, Y., Xia, Q., Wang, H., Li, Z., 2015. Vapor-enhanced CO_2 adsorption mechanism of composite PEI@ZIF-8 modified by polyethyleneimine for CO_2/N_2 separation. Chem. Eng. J. 280, 363–369.
Xu, C., Cheng, Z., 2021. Thermal stability of ionic liquids: current status and prospects for future development. Processes 9, 337.
Yousef, A.M., El-Maghlany, W.M., Eldrainy, Y.A., Attia, A., 2018. New approach for biogas purification using cryogenic separation and distillation process for CO_2 capture. Energy 156, 328–351.
Yousef, S., Šereika, J., Tonkonogovas, A., Hashem, T., Mohamed, A., 2021. CO_2/CH_4, CO_2/N_2 and CO_2/H_2 selectivity performance of PES membranes under high pressure and temperature for biogas upgrading systems. Environ. Technol. Innov. 21, 101339.
Zhang, X., Zhang, T., Wang, Y., Li, J., Liu, C., Li, N., Liao, J., 2018. Mixed-matrix membranes based on Zn/Ni-ZIF-8-PEBA for high performance CO_2 separation. J. Membr. Sci. 560, 38–46.
Zhao, D., Ren, J., Li, H., Hua, K., Deng, M., 2014. Poly(amide-6-b-ethylene oxide)/SAPO-34 mixed matrix membrane for CO_2 separation. J. Energy Chem. 23, 227–234.
Zheng, W., Ding, R., Yang, K., Dai, Y., Yan, X., He, G., 2019. ZIF-8 nanoparticles with tunable size for enhanced CO_2 capture of Pebax based MMMs. Sep. Purif. Technol. 214, 111–119.
Zhu, C., Peng, Y., Yang, W., 2021. Modification strategies for metal-organic frameworks targeting at membrane-based gas separations. Green Chem. Eng. 2, 17–26.
Zoubeik, M., Mohamedali, M., Henni, A., 2016. Experimental solubility and thermodynamic modeling of CO_2 in four new imidazolium and pyridinium-based ionic liquids. Fluid Phase Equilibria 419, 67–74.